Next-Generation Cryo-Electric Hydrogen-Powered Aviation

A Disruptive Superconducting Propulsion System Cooled by Onboard Cryogenic Fuels

Abstract

The idea of hydrogen-powered airplanes has recently attracted a revitalized push in the aviation sector to combat CO_2 emissions. However, to also reduce, or even eliminate, non-CO_2 emissions and contrails, the combination of hydrogen with all-electric solutions is undoubtedly the best option. This article explores the next wave of disruptive technological developments needed to scale up zero-emission aviation beyond 2035. With respect to conventional electrical propulsion, major breakthroughs will be needed in terms of reducing the voltage level while increasing system-level power density and overall efficiency. We show how a next-generation hydrogen-powered aircraft could take advantage of its onboard cryogenic fuels to cool the electrical components, enabling a cryo-electric superconducting drivetrain that could lead to extraordinary performances.

Figure 1: *Conceptual airplane with fuselage-integrated fuel cells and LH_2 tanks and additional wing-embedded LH_2 tanks.*

Introduction

Conventional aircrafts rely heavily on energy-dense fuels, where strict weight and certification requirements apply. Until recently, it has been a challenging task to transform the aviation industry into more sustainable alternatives. A major limitation has been that batteries are very heavy and energy-dilute, which makes them only applicable as an energy source for smaller commuter aircraft. However, a paradigm shift is now occurring, where aerospace industries and stakeholders consider hydrogen (H_2) fuel as a renewable surrogate onboard the aircraft [1].

Powering an aircraft with hydrogen is not a new idea. Hydrogen is, in many ways, an ideal aviation fuel, not only because it is CO_2-free. It is the smallest element in the periodic table and the lightest energy carrier of any non-nuclear fuel. It can either be burnt in a combustion engine or be used to power fuel cells that enable electrical propulsion.

While gaseous hydrogen (GH_2) is already low in mass, it needs a lot of space to be stored. Compressed hydrogen (200-700 bar) is one alternative, but it is not the most space-efficient solution. Liquid hydrogen (LH_2) at 20 K and 1 bar can further reduce the volume by 50 percent [2], which allows the airplane to hold significantly more fuel. However, for the same energy, LH_2 still occupies about five times the space compared to conventional jet fuel [2].

In traditional tube and wing airframes, the increased volume required by hydrogen storage represents a major challenge. LH_2 tanks available today are either spherical or cylindrical and must be placed in the fuselage, reducing space for passengers and luggage. The main argument for using such tanks is that they have low surface areas, yielding low boil-off rates of around 1.5 % per day [3]. However, an aircraft's predictable fuel consumption pattern allows boil-off to be directly used as fuel, as one only needs to store the LH_2 for hours at a time. Hence, tanks with shapes customized to fit inside the innermost part of the wing (see Figure 1) should also be considered to reduce the size of fuselage-integrated tanks while improving system redundancy. Still, wing-embedded tanks will pose additional challenges regarding icing, structural strength, and inspection difficulties. The storage issues could be handled in the long term by developing completely new airframe designs such as the blended wing, which would grant a larger aircraft volume with a higher fuel efficiency [4].

The most efficient and climate-friendly solution for hydrogen-power aircraft is to go for fully electric propulsion, but overall, this solution is very mass-intensive. However, the onboard cryogenic fuels could significantly help deal with this major issue. As LH_2 cannot be utilized directly in fuel cells but need to be brought from liquid to a gas at about 350 K, large amounts of heat must be added to the fuel. Thus, a synergy can be made from this otherwise wasted cryogenic refrigeration power to enable a superconducting propulsion system, including superconducting machines (SCMs) and cold power electronics (CPE). These are low-hanging fruits that could lead to radical space and weight reductions onboard the aircraft. Such opportunities can be realized without having to pay the price, nor the volume occupation and mass needed for the cooling equipment usually needed to achieve these extraordinary performances. In fact, this ground-breaking synergy makes cryogenic energy conversion systems relevant

in a whole new way for aviation. The SCMs can become a wildcard technology of more than five times higher power densities than their conventional counterparts.

SCMs have lately been proposed in aviation to be at least five times power-dense than existing solutions (i.e., 25 kW/kg and beyond), but it overlooks the SCMs' inherently energy- and weight-intensive cryogenic cooling needs. Contrary to this limitation, a new class of SCMs can be enabled using the LH_2 fuel onboard the aircraft as a cryogenic cooling medium [5]. Also in gas form, hydrogen is a widely used coolant, especially at higher temperatures [6, 7]. Moreover, hydrogen needs to hold at least 60 °C when consumed in fuel cells, which means it has to be boiled and heated on its way from the tank. This need creates a synergy where there are new achievable breakthroughs in performance of utilizing the direct cooling capacity of hydrogen to enable:

- ✓ SCMs cooled at temperatures between 20 K and 60 K;
- ✓ High-temperature superconducting (HTS) AC and DC cables chilled at ~ 80 K; and,
- ✓ Cold power electronics (CPE) operating at ~ 160 K.

In order to utilize most of the high-value cryogenic properties of the hydrogen fuel, taking advantage of a wide enough temperature span, the components should be operated and designed for different temperature intervals, optimizing the overall system performance. By providing the coldest H_2 for the SCMs first, their power density enhances significantly when heavy cryocoolers are avoided (see Figure 2 for simplified drawing).

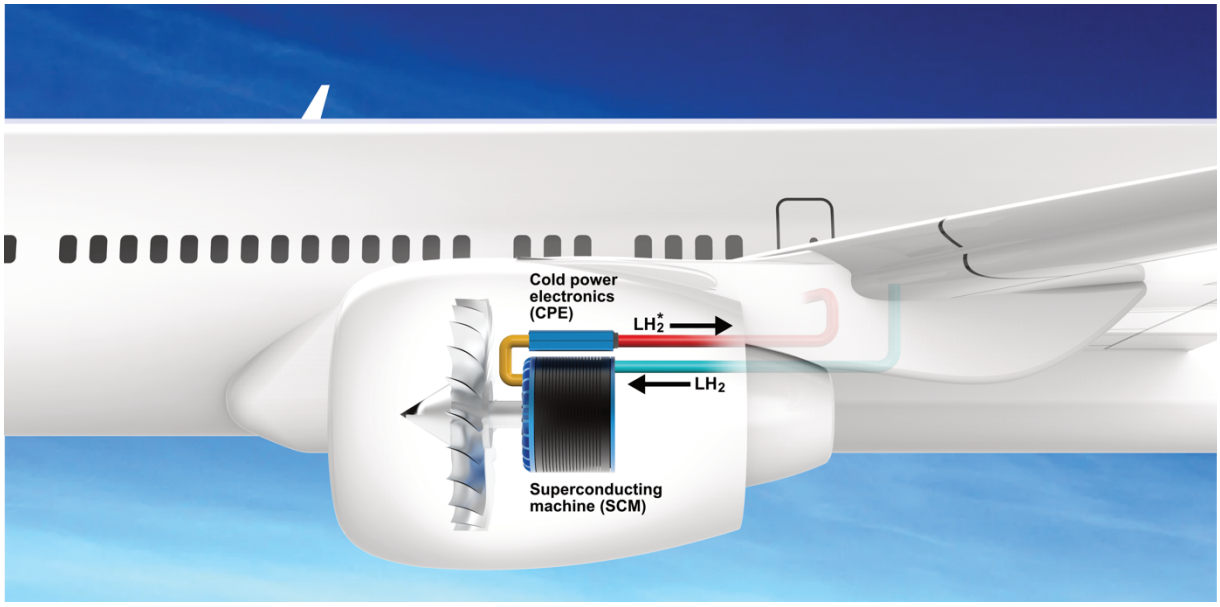

Figure 2: *Hydrogen-cooled superconducting machine and cold power electronics inverter (outgoing LH_2* is no longer liquid).*

Important Contributions to the Core Technologies

The key challenges in realizing cryo-electric hydrogen-powered aviation in the future involve maturing the individual components in the superconducting propulsion system, but it also requires sufficient advancements in the distribution and heat exchange of the cold hydrogen in the envisaged cryogenic loop. The emphasis must not only be on the functional requirements. Even more important are the safety requirements. An issue here is that existing aircraft safety standards are not aimed at drivetrains based on hydrogen and superconductors. It, therefore, seems unlikely that any cryo-electric hydrogen-powered aircraft can fully comply with existing standards and regulations. Consequently, we are looking at a very demanding process to align standards and technology within this field.

It should be emphasized that conventional electrical technology is not even close to approaching the performances of superconducting solutions. By sophisticated lightweight construction techniques, the most power-dense permanent magnet machine achieves a power density of 5.2 kW/kg (i.e., 260 kW, 2500 rpm, 50 kg direct-driven motor demonstrated by Siemens in 2015). However, it is still too heavy to be used for multi-megawatt electric propulsion [8]. In fact, a turbo-electric retrofit for a 100-seater aircraft requires an electric machine power-to-weight (PTW) ratio of at least 16 kW/kg [9], compatible with SCMs 20 kW/kg and beyond [10].

Despite the fact that superconductors can be operated lossless under DC conditions (efficiency $\approx$ 100 %), they do generate loss under AC conditions (efficiency $\leq$ 99.9 %) [11]. This is the case both when the current in the superconductor is time-varying and if the superconductors are exposed to an external AC field. These losses must be removed from the superconductors so that the operating temperature under no circumstances exceeds the critical temperature (T_c), where the material ceases to be superconducting. It varies for different superconductors, where REBCO has $T_c \approx 90$ K, and MgB_2 has $T_c \approx 40$ K at ideal operating conditions.

Although keeping the superconductors safely below T_c is imperative, there are significant gains to be achieved by operating them even further below this temperature. The current loading can be increased significantly as the temperature is decreased. SCMs chilled by LH_2 at 20 K can achieve a much higher power density than a motor chilled by liquid nitrogen (LN_2) at 64 K (e.g., up to 5 times) [11]. However, one must also consider the cooling penalty; a conventional cryocooler consumes as much as 100 W to remove 1 W of heat at 20 K, considering the ideal Carnot cycle and an efficiency of the cooling machine of 15 %. This penalty is proposed to be mitigated by utilizing the onboard cryogenic fuel, replacing the need for heavy and inefficient cryocoolers while enabling better SCMs.

During the phase shift from liquid to gaseous hydrogen, the temperature remains at 20 K until it has absorbed enough heat to be fully evaporated. After that, it is still a very efficient cryogenic gas that can remove a lot of heat from superconducting components, but the gas temperature will creep upwards during the heat removal process. For demanding components, such as MgB_2 superconductors ($T < 25$ K), it is important to ascertain that the maximum operating temperature does not exceed the permissible maximum temperature.

The regional flight segment is seen by many as the right market to introduce cryogenic superconducting technologies [2]. An aircraft in this segment carries up to 80 passengers for distances up to approximately 1000 km. We are looking at peak propulsive power in the range between 1 to 5 MW. Therefore, the new focus on zero-emission aviation at scale demands at least 1 MW and up to 5 MW of rated power in the electric motors. Herein, the machine's efficiency and power density are the key figures-of-merit to pave the way to cleaner aviation in regional flights and beyond.

Superconducting Machines (SCMs)

In conventional electrical machines, the electrical conductors are considered as the main source of losses. Therefore, superconductors are promising in this context. Early SCMs were synchronous machines using superconducting DC field windings only. However, to push it further, the EU-funded project ASuMED was set up to develop and test the first aerospace-grade fully superconducting motor [12], where the stator uses LH_2 and the rotor gaseous helium (GHe). ASuMED aimed at a 1-MW, 6000-rpm, 400-Hz, 4.95-kA propulsion motor with a machine efficiency beyond 99.9 % and a machine mass target of 50-kg, yielding a power density of 20 kW/kg [13]. It was intended to be suitable for hybrid-electric distributed propulsion (HEDP) in future aviation. Later, another fully superconducting 10.5-MW, 3500-rpm, 350-Hz, 7-kA was reported with an efficiency of 99.92 % and a total mass of 303 kg, achieving a power density as high as 34.7 kW/kg [14].

The ASuMED rotor utilized stacked superconductors that basically function as permanent magnets with high remanent flux density and are therefore premised on the basis that the overall power density favors a high air-gap flux density that cannot be obtained by passive permanent magnets (PMs). Superconducting magnets can be more than 10 times stronger than conventional ones but are continuously being pushed further, as shown by the recent world record of 17.9 T [15]. However, these magnets are not suited for electrical machines, where a maximum of 3 T is usually considered within the feasible range.

The main drawback of the ASuMED demonstrator is the fact that a high flux density from the rotor often breaks the saturation limit of the core [16], which in turn increases the weight of the machine. However, it provided the next step to make the AC windings in the stator superconducting as well. The main rationale for the ASuMED project was the fact that the option of a fully superconducting machine is far from a mature technology [17].

A more robust option is to solely focus on making the stator AC-windings superconducting instead. These windings are static and easier to cool for the cryogenic system. Moreover, recent studies on fully superconducting SCMs show that they are often optimized to be lightweight at air gap magnetic flux densities below 0.9 T [18]. This can be understood by the fact that higher flux densities cause the machine's core to saturate if not more iron material is added, which also adds to the overall weight. For the rotor part, PMs can achieve a remanent magnetization of up to 1.3 T, which appears to be sufficient in many cases.

An alternative solution to set up the magnetic field from the rotor is to use PMs and arrange them in a Halbach array. Such a configuration avoids the need for magnetic iron parts in the rotor, which has the potential for further reductions in the active weight. PMs are also considered a reliable magnetic source to provide safe torque generation in general aviation systems, as they are not dependent on active components [19]. Figure 3 depicts the different configurations discussed and briefly compares them. The iron around the cryocooled slots makes it easier to transmit the fully developed torque from the armature winding [20]. Concentrated windings are assumed in the stator to reduce the usage of AC superconductors, and to reduce the number of slots where cryogenic cooling is needed.

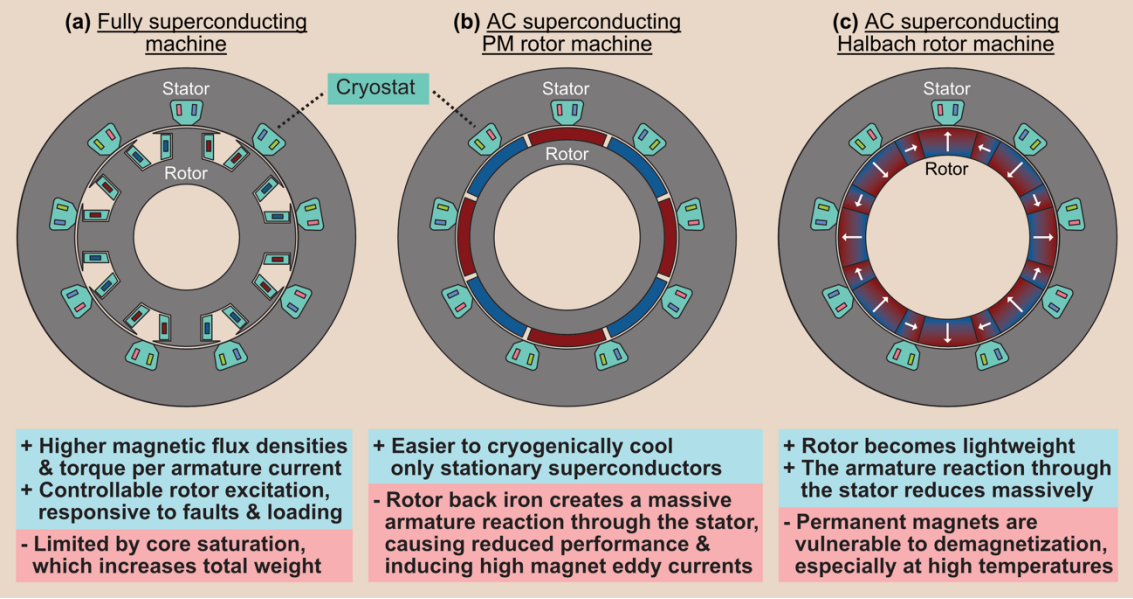

Figure 3: *Power-dense superconducting machine topologies relevant for cryo-electric hydrogen-powered aviation.*

Cold and Cryogenic Power Electronics (CPE)

The existing research has already reported the potential of cold and cryogenic power electronics (CPE), where there are mainly two considerations supporting their use. Lowering the operational temperature improves the performance, while one omits huge leads that would be needed to feed the current from the warm to the cryogenic parts of the propulsion system. One also allows a continuous cooling loop of the cryogenic medium. The power electronics devices are traditionally warm components in cryogenic power systems, which causes significant heat leaks to adjacent cryogenic components.

CPE has earlier been proposed to increase the power density of energy conversion systems [21]. Silicon MOSFET switching devices have already shown efficiency improvements when running at cryogenic temperatures (77 K) [22]; however, that is still not the case for Silicon Carbide (SiC) MOSFETs [23]. At

switching frequencies of 140 kHz, a cryogenic 40-kW three-level NPC inverter showed 30 percent less losses than at room temperature [24]. Moreover, the operation of Gallium Nitride (GaN) power devices has been demonstrated over a temperature range from 400 K and down to 4.2 K, allowing high operational flexibility [25]. GaN devices have also been shown to have an overload current capability of four times the rated capacity when cryogenically cooled [26]. Already at 213 K, a single-phase 1-kW GaN inverter at 60 Hz load frequency exhibited a 16 percent reduction in losses compared to room temperatures [27]. A myriad of similar observations also makes a case for the recent trend of CPE, proposing an operating temperature of about 160 K.

As the operating temperature drops, power electronic devices can be utilized with minimal resistive losses, ensuring excess heat load into the wider system is kept to a minimum. It also increases the permissible current loading, leading to higher power to weight ratios. Besides a direct reduction in volume and weight, the efficiency increase of the CPE leads to lower requirements for heat removal. In the case of hydrogen-electric aircraft, it translates to using H_2 for other high-value cooling purposes as well. Figure 4 depicts and compares the two most common proposed CPE inverter topologies.

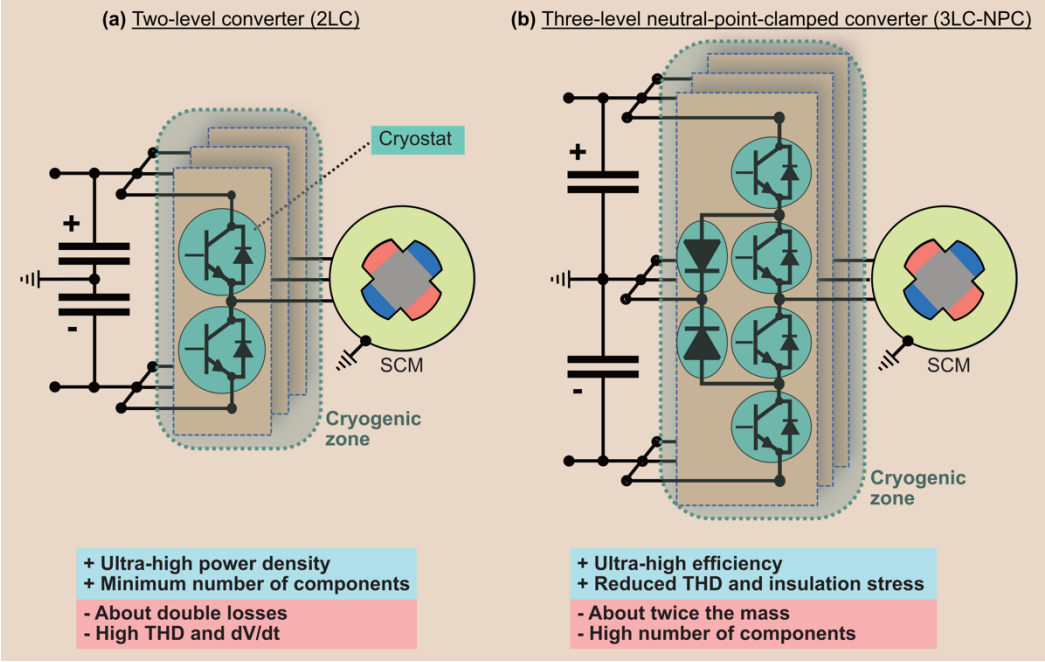

Figure 4: *Comparison of the two commonly proposed cryogenic power electronic converters for feeding SCMs based on* [14].

Combining Cold Power Electronics and Superconducting Machines

The recently proposed ASCEND project introduces a propulsion system demonstrator, as depicted in Figure 5. The overall targets for each component and the desired figure-of-merit for the end product are

provided in Table 1 and compared against 2030 targets. The first goal is to reach a system efficiency 5-6 % better than conventional technology. Table 1 shows that taking all electrical components into account adds significant mass and heat loss penalties to the overall system configuration. As a result, more realistic values for the system's power density and overall efficiency can be identified. These additional inefficiencies occurring throughout the system would add additional cooling needs and heat exchange mass if these losses could not be handled by synergizing the hydrogen fuel distribution system of LH_2 with the cooling system. One would also want to utilize the whole temperature span of the LH_2 before the H_2 is utilized in fuel cells, which makes the case for different temperature zones, as depicted in Figure 5. However, it adds challenges to the electrical interconnections, in which heat leakage will inevitably occur. The connectors should be strategically designed to limit these parasitic effects and to make the system easy to inspect.

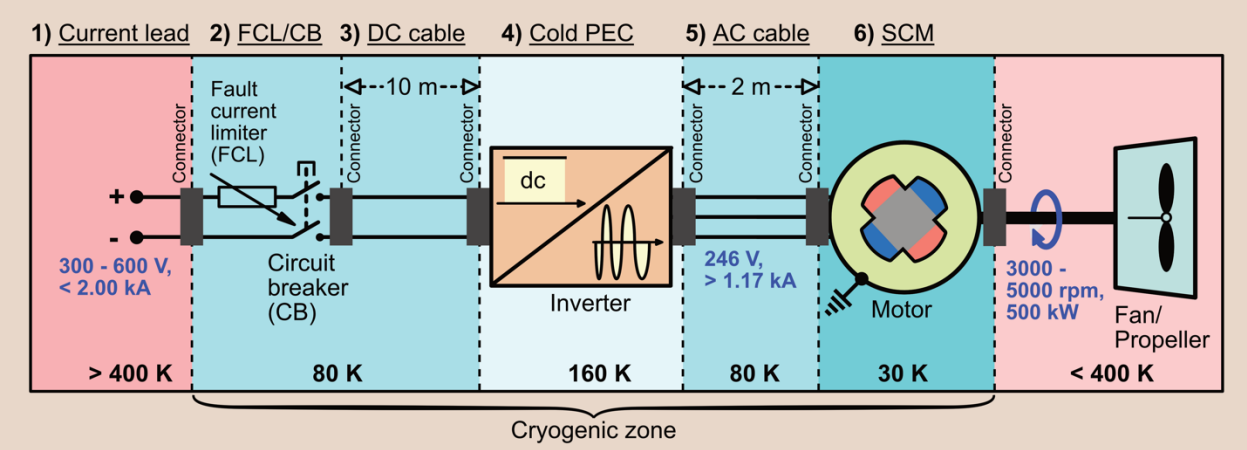

Figure 5: *Cryogenic zone classification of ASCEND's 0.5-MW demonstrator including connectors.*

Table 1: *ASCEND demonstrator's figure-of-merits for the 0.5-MW (Courtesy of Airbus UpNext) vs. 2030 targets, neglecting SCM reactive power needs, if any. The torque density targets of the 5000-rpm SCM corresponds to > 21.22 Nm/kg and 38.20 Nm/kg.*

Component	TRL6 before	Comp. mass	Power density	Power input	Heat loss	Power output	Comp. efficiency
1) Current lead (CL)	2023	≤ 5 kg	≥ 101.78 kW/kg	≤ 509.10 kW	≤ 0.20 kW	≤ 508.90 kW	≥ 99.96 %
	2030	≤ 3 kg	≥ 168.23 kW/kg	≤ 504.80 kW	≤ 0.10 kW	≤ 504.70 kW	≥ 99.98 %
2) Fault current limiter (FCL) + circuit breaker (CB)	2023	≤ 10 kg	≥ 50.87 kW/kg	≤ 508.90 kW	≤ 0.20 kW	≤ 508.70 kW	≥ 99.96 %
	2030	≤ 5 kg	≥ 100.92 kW/kg	≤ 504.70 kW	≤ 0.10 kW	≤ 504.60 kW	≥ 99.98 %
3) HTS DC cable (10 meter) + 2x connectors	2023	≤ 25 kg	≥ 20.34 kW/kg	≤ 508.70 kW	≤ 0.10 kW	≤ 508.60 kW	≥ 99.98 %
	2030	≤ 20 kg	≥ 25.23 kW/kg	≤ 504.60 kW	≤ 0.05 kW	≤ 504.55 kW	≥ 99.99 %
4) Cold power electronics (CPE) + filters	2023	≤ 35 kg	≥ 14.36 kW/kg	≤ 508.60 kW	≤ 6.00 kW	≤ 502.60 kW	≥ 98.82 %
	2030	≤ 16 kg	≥ 31.35 kW/kg	≤ 504.55 kW	≤ 3.00 kW	≤ 501.55 kW	≥ 99.41 %
5) HTS AC cable (2 meter) + 2x connectors	2023	≤ 11 kg	≥ 45.68 kW/kg	≤ 502.60 kW	≤ 0.10 kW	≤ 502.50 kW	≥ 99.98 %
	2030	≤ 6 kg	≥ 83.58 kW/kg	≤ 501.55 kW	≤ 0.05 kW	≤ 501.50 kW	≥ 99.99 %
6) Direct-drive 5000-rpm SCM	2023	≤ 45 kg	≥ 11.11 kW/kg	≤ 502.50 kW	≤ 2.50 kW	500.00 kW	≥ 99.50 %
	2030	≤ 25 kg	≥ 20.00 kW/kg	≤ 501.50 kW	≤ 1.50 kW	500.00 kW	≥ 99.70 %
Overall system	2023	≤ 131 kg	≥ 3.82 kW/kg	≤ 509.10 kW	≤ 9.10 kW	500.00 kW	≥ 98.21 %
	2030	≤ 75 kg	≥ 6.67 kW/kg	≤ 504.80 kW	≤ 4.80 kW	500.00 kW	≥ 99.05 %

The overall power density of the drivetrain targeted in Table 1 can be verified with the following calculation

$$p_{tot} \approx \frac{1}{\frac{1}{p_1}+\frac{1}{p_2}+\frac{1}{p_3}+\frac{1}{p_4}+\frac{1}{p_5}+\frac{1}{p_6}},$$

where, p_1, p_2, etc., are power densities of each electrical component and p_{tot} is the power density of the overall system. This formula assumes that all components in the system have the same power rating, so it should be used with caution if the system contains components with poor efficiencies or if the components are not arranged in series. For the overall power densities in Table 1, the formula yields 3.84 kW/kg and 6.70 kW/kg, which is an overestimation of 0.4 % and 0.5 %, respectively.

It can be clearly seen from Table 1 that the overall PTW is around 70 % lower than the power density of SCMs. Moreover, the table indicates that the SCM has the lowest PTW. It is, therefore, the most important component to improve further.

Superconducting Distribution and Storage

The DC-link is an essential part of the propulsion chain to transfer the energy from the power sources to the machine-side converter. A voltage level below 500 V is needed to improve safety and installation issues. In such a direct current distributions system, fault management is much more challenging in operation due to the absence of zero-crossings in the current, which will be worsened by the low impedance of the superconducting powertrain. Developing electrical protection is key, including fault detection capability, reliable fault current limiters (FCLs) and fast-operating circuit breakers (CBs). It is also important to make them superconducting, reducing the size and improving their efficiency.

To control the DC-link, batteries would be needed to peak-shave the dynamics of the propulsion chain and decouple the dynamics of the fuel cell. Here, superconducting magnetic energy storage (SMES) could play a role as a replacement for batteries. SMES is beneficially high in power density and efficiency but more moderate in energy density.

A Direct Hydrogen-Cooled Superconducting Propulsion System

To move beyond the projects of ASuMED and ASCEND, further system-level improvements are needed, which are not merely focusing on the drivetrain segment of the system. These steps are described in the conceptual system outlined in Figure 6.

To make ultra-compact SCMs, it is necessary to operate the superconductors with alternating currents at higher frequencies. Such operation generates small amounts of heat losses which must be promptly removed from the superconductors. LH_2 is well suited to do this job due to its high heat capacity and low temperature. There is also ample cooling capacity left in the hydrogen after the heat has been removed from the SCM. When raising the hydrogen's temperature from 20 K to 300 K, the available cooling capacity corresponds to about 2.8 % of its energy content (higher heating value), including the phase change at 20 K. The cooling capacity should not be confused with the chemical energy contained in the fuel since it comes as an extra feature. However, the 2.8 % ratio emphasizes the scalability of the concept, and that the hydrogen may be used as a coolant not only for the SCM, but also other cryogenic components. Figure 6 shows how the hydrogen zigzags through all of these components before it is consumed as fuel in the PEM fuel cell.

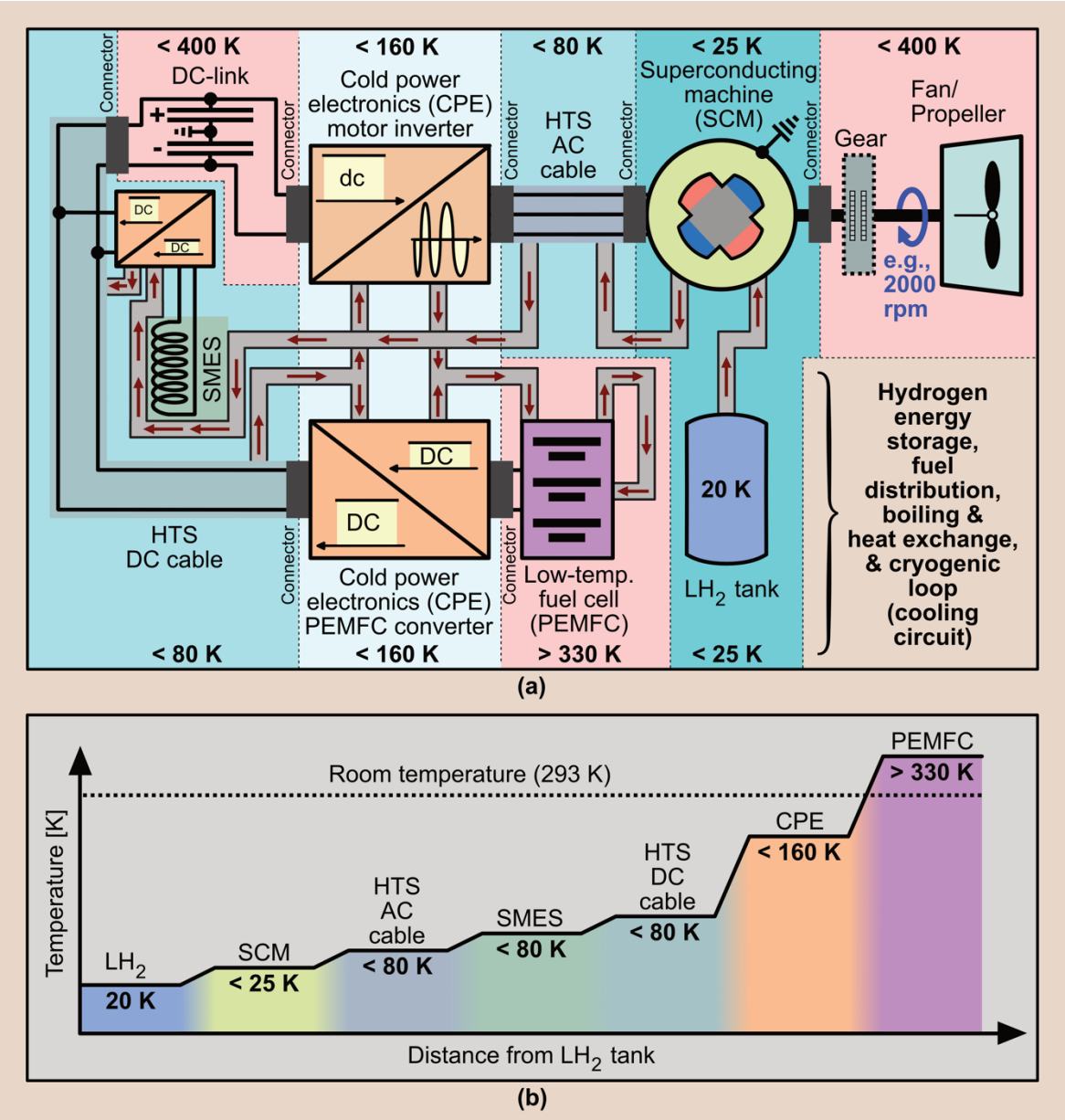

Figure 6: *Sketch of a proposed architecture with cryogenic zone arrangement of a direct hydrogen-cooled propulsion system including heat exchange circuit.* ***(a)****: Cryogenic loop diagram.* ***(b)****: Thermal path of the hydrogen.*

System-Level Mass and Inefficiency Savings

To provide an estimation of the potential savings in the SCM, taking advantage of the system synergies proposed in Figure 6, the overall efficiency and power density of SCMs, including the effect of the cryocooler, must be accurately considered. The electrical power consumed by a cryocooler (P_{cryo}) depends on the cryocooler efficiency (η_{cryo}), the ambient temperature (T_{amb}), the cryogenic temperature (T_{cryo}), and the SCM's AC losses ($P_{loss,AC}$) as follows.

$$P_{cryo} = \frac{1}{\eta_{cryo}} \cdot \underbrace{\frac{T_{amb} - T_{cryo}}{T_{cryo}}}_{1/COP} \cdot P_{loss,AC}$$

Taking the additional power needs (P_{cryo}) and the overall SCM losses ($P_{loss,tot}$) into account, with P_{scm} as the mechanical power of the SCM, the overall efficiency (η_{tot}) is reduced, yielding:

$$\eta_{tot} = \frac{P_{scm}}{P_{scm} + P_{loss,tot} + P_{cryo}}$$

What is implied in this overall efficiency is not only the losses in the SCM itself but also the additional electrical power needed for cryocooling (i.e., P_{cryo}) in the fully electrified aircraft, where extra fuel cell stack-mass would be required. Thus, eliminating P_{cryo} makes the potential savings even better.

Table 2: *Overall system considerations of a direct-drive 1.0-MW SCM comparing the performance with cryocooler against hydrogen cooling. Assumptions include 25 K cryogenic temperature (T_{cryo}) and 300 K ambient temperature (T_{amb}) at sea level.*

Parameter	Symbol	w/ cryocooler	w/ direct hydrogen cooling
SCM efficiency	η_{mach}	99.7 %	99.7 %
SCM power density	P_{scm} / m_{mach}	12.5 kW/kg – 25.0 kW/kg	12.5 kW/kg – 25.0 kW/kg
SCM total heat losses	$P_{loss,tot}$	3.0 kW	3.0 kW
SCM AC losses	$P_{loss,AC}$	2.0 kW	2.0 kW
Cryocooler efficiency [28]	η_{cryo}	15 % – 30 %	~ 100 %
Cryocooler mass per power loss removal [28]	m_{cryo} / P_{cryo}	3 kg/kW	~ 0 kg/kW
Cryocooler mass per propulsion power	m_{cryo} / P_{scm}	0.22 kg/kW – 0.44 kg/kW	~ 0 kg/kW
Cryocooler power	P_{cryo}	73.33 kW – 146.67 kW	~ 0 kW
Cryocooler mass	m_{cryo}	220 kg – 440 kg	~ 0 kg
SCM mass	m_{scm}	40 kg – 80 kg	40 kg – 80 kg
Total mass of SCM + cryocooler	m_{tot}	260 kg – 520 kg	40 kg – 80 kg
Cryocooler mass contribution	m_{cryo} / m_{tot}	73.3 % – 91.7 %	~ 0 %
Overall efficiency	**η_{tot}**	**87.0 % – 92.9 %**	**~ 99.7 %**
Overall power density	**P_{scm} / m_{tot}**	**1.92 kW/kg – 3.85 kW/kg**	**12.5 kW/kg – 25.0 kW/kg**

Table 2 outlines the calculation of the overall power density and efficiency for a 1.0-MW direct-drive SCM for regional flight, when the mass and power consumption of the cryocooler is also considered and compared against the concept of direct hydrogen cooling. It highlights the fact that the overall efficiency is between 6.8 and 12.7 percent lower than the efficiency of the SCM (i.e., 99.7 %), which is significant considering the additional energy needed onboard the aircraft to compensate for the inefficiency. The main SCM components are included. Piping and structural materials come in addition.

In addition, the power density, including the cryocooler, is lower than 3.85 kW/kg, which is comparable to the most power-dense conventional non-superconducting machines, even though the power density of SCM itself is considered to be higher than 12.5 kW/kg. The cryocooler dramatically reduces the PTW ratio of cryocooled SCMs by at least 69.2 percent. Earlier studies [29, 30] report that the mass of the cryocoolers can constitute as much as 70 percent of the total mass of the electric propulsion system.

From a holistic perspective, the SCM solution with cryocooler is rendered unfeasible due to its low efficiency and power density. Therefore, the only way to utilize the superior performance of the SCM is through other approaches such as direct hydrogen cooling, as proposed in this paper.

Conclusions

This article has proposed a future wildcard concept for next-generation cryo-electric propulsion systems in zero-emission hydrogen-powered aviation. In particular, we showcase the potential implications of enhancing the SCM's power density, as it is found to be the most limiting component in the drivetrain segment in terms of mass and space occupation. Moreover, we emphasize significant system-level improvements found in using onboard cryogenic fuels onboard as a cooling medium, enabling an important synergy. By taking advantage of a cryogenic loop sweeping through the whole superconducting propulsion system, there is an extraordinary potential for massive weight and inefficiency savings found at the multi-megawatt level.

Even though the outlined system-level approach is promising in terms of exceptional performance gains, the apparent challenges cannot be underestimated. It is, therefore, essential to demonstrate that such systems can be maintained superconducting and at cryogenic temperatures in future demonstrations. Here, one must show that it is possible to extract heat loss from the electrical system while simultaneously managing failures and faults in both the electrical and cryogenic systems.

Acknowledgements

The work was supported in part by the GREAT project, *GReen Aviation Technologies*, which is one out of seven short-listed proposals that bring an expression of new ideas incorporated into the European Partnership for Clean Aviation (launched December 1st, 2021). It was developed in 2020 as a consortium between the Norwegian University of Science and Technology (NTNU), SINTEF Energy Research, and the

SINTEF Group. GREAT focuses on the development of technologies to increase the performance/reliability of electrical components and optimize the efficiency of hydrogen-based propulsion systems using superconducting power components. In particular, the authors gratefully acknowledge the support of SINTEF ER, especially Niklas Magnusson, who provided important inputs to the manuscript from the field of superconductivity. In addition, thanks to Ida Hjorth for helping out with her expertise in gas technology and chemical engineering.

Biographies

Jonas Kristiansen Nøland (jonas.k.noland@ntnu.no) earned his Ph.D. degree in engineering physics from the Ångström Laboratory, Uppsala University, Uppsala, Sweden, in 2017. He is currently an Associate Professor in the Department of Electric Power Engineering (IEL) at the Norwegian University of Science and Technology (NTNU), Trondheim, Norway, where he focuses on scaling up zero-emission propulsion systems. Dr. Nøland is a Senior Member of the IEEE and the IES, and is currently serving as an associate editor of *IEEE Transactions on Industrial Electronics* and an editor of *IEEE Transactions on Energy Conversion*.

Runar Mellerud (runar.mellerud@ntnu.no) is currently pursuing a Ph.D. degree focusing on superconducting electrical machines for aerospace at the Norwegian University of Science and Technology (NTNU), Trondheim, Norway.

Christian Hartmann (christian.hartmann@ife.no; christian.hartmann@ntnu.no) is pursuing a Ph.D. degree focusing on cryo-electric propulsion systems for next-generation aviation at the Norwegian University of Science and Technology (NTNU), Trondheim, Norway. He is currently a Senior Scientist at the Institute for Energy Technology (IFE), Halden, Norway.

References

[1] "*Hydrogen-powered aviation: A fact-based study of hydrogen technology, economics, and climate impact by 2050*," Fuel Cells & Hydrogen Joint Undertaking, Brussels, Belgium, May 2020 [Online], URL: https://www.fch.europa.eu/sites/default/files/FCH Docs/20200720_Hydrogen Powered Aviation report_FINAL web.pdf

[2] J.K Nøland, "*Hydrogen Electric Airplanes: A disruptive technological path to clean up the aviation sector*", IEEE Electrification Magazine, vol. 9, no. 1, pp. 1-11, 2021, URL: https://ieeexplore.ieee.org/document/9371235

[3] K. Verfondern, *et. al.*, "*Handbook of Hydrogen Safety*" (Chapter on LH_2 Safety, pp. 18), PRESLHY, Fuels Cells and Hydrogen (FCH) Joint Undertaking, 2021, URL: https://hysafe.info/wp-content/uploads/sites/3/2021/04/D39_2021-01-PRESLHY_ChapterLH2-v3.pdf

[4] "*Blended Wing Body – A potential new aircraft design*" (Chapter on LH_2 Safety, pp. 18), NASA, URL: https://www.nasa.gov/centers/langley/news/factsheets/FS-2003-11-81-LaRC.html

[5] H. Karmaker, *et. al.*, "*High power density superconducting rotating machines – Development status and technology roadmap*," Superconductor Science and Technology, vol. 30, no. 12, 2017, URL: https://iopscience.iop.org/article/10.1088/1361-6668/aa833e/meta

[6] J. Han, *et. al.*, "*Influence of Electric Shield Materials on Temperature Distribution in the End Region of a Large Water–Hydrogen–Hydrogen-Cooled Turbogenerator*," IEEE Transactions on Industrial Electronics, vol. 67, no. 5, May 2020, URL: https://ieeexplore.ieee.org/document/8736046

[7] L. Weili, *et. al.*, "*Calculation of Ventilation Cooling, Three-Dimensional Electromagnetic Fields, and Temperature Fields of the End Region in a Large Water–Hydrogen–Hydrogen-Cooled Turbogenerator*," IEEE Transactions on Industrial Electronics, vol. 60, no. 8, Aug. 2013, URL: https://ieeexplore.ieee.org/document/6211416

[8] M. Filipenko, *et. al.*, "*Concept design of a high power superconducting generator for future hybrid-electric aircraft*," Superconductor Science and Technology, vol. 33, no. 5, March 2020, URL: https://iopscience.iop.org/article/10.1088/1361-6668/ab695a

[9] B. Lukasik, *et. al.*, "*Turboelectric distributed propulsion system as a future replacement for turbofan engines*," Proc. ASME Turbo Expo, no. GT2017-63834, V001T01A017, Aug. 2017, URL: https://asmedigitalcollection.asme.org/GT/proceedings/GT2017/50770/V001T01A017/291323

[10] Y. Terao, *et. al.*, "*Lightweight Design of Fully Superconducting Motors for Electrical Aircraft Propulsion Systems*," IEEE Transactions on Applied Superconductivity, vol. 29, no. 5, Aug. 2019, URL: https://ieeexplore.ieee.org/document/8654678

[11] R. Sugouchi, *et. al.*, "*Conceptual Design and Electromagnetic Analysis of 2 MW Fully Superconducting Synchronous Motors With Superconducting Magnetic Shields for Turbo-Electric Propulsion System*," IEEE Transactions on Applied Superconductivity, vol. 30, no. 4, June 2020, URL: https://ieeexplore.ieee.org/document/9001263

[12] "*ASuMED: System topology report*," H2020 project delivery report, grant no. 723119, Oct. 2017, URL: http://asumed.oswald.de/images/pdf/ASuMED_D1.2_system-topology-report.pdf

[13] F. Grilli, *et. al.*, "*Superconducting motors for aircraft propulsion: the Advanced Superconducting Motor Experimental Demonstrator project*," Journal of Physics: Conference Series, no. 1590, 2020, URL: https://iopscience.iop.org/article/10.1088/1742-6596/1590/1/012051/pdf

[14] M. Boll, *et. al.*, "*A holistic system approach for short range passenger aircraft with cryogenic propulsion system*," Superconductor Science and Technology, vol. 33, no. 044014, 2020, URL: https://iopscience.iop.org/article/10.1088/1361-6668/ab7779/pdf

[15] M. Zhang, "*A new world record for a superconducting trapped field magnet*," Superconductor Science and Technology, vol. 32, no. 7, June 2019, URL: https://iopscience.iop.org/article/10.1088/1361-6668/ab17e6

[16] T. Qu, *et. al.*, "*Development and testing of a 2.5 kW synchronous generator with a high temperature superconducting stator and permanent magnet rotor*," Superconductor Science and Technology, vol. 27, no. 7, March 2014, URL: https://iopscience.iop.org/article/10.1088/0953-2048/27/4/044026

[17] C. D. Manolopoulos, *et. al.*, "*Stator Design and Performance of Superconducting Motors for Aerospace Electric Propulsion Systems*," IEEE Transactions on Applied Superconductivity, vol. 28, no. 4, June 2018, URL: https://ieeexplore.ieee.org/document/8310968

[18] M. Corduan, *et. al.*, "*Topology Comparison of Superconducting AC Machines for Hybrid Electric Aircraft*," IEEE Transactions on Applied Superconductivity, vol. 30, no. 2, March 2020, URL: https://ieeexplore.ieee.org/document/8947911

[19] P. Masson, *et. al.*, "*Safety Torque Generation in HTS Propulsion Motor for General Aviation Aircraft*," IEEE Transactions on Applied Superconductivity, vol. 17, no. 2, June 2007, URL: https://ieeexplore.ieee.org/document/4277589

[20] C. D. Manolopoulos, *et. al.*, "*Comparison Between Coreless and Yokeless Stator Designs in Fully-Superconducting Propulsion Motors*," IEEE Transactions on Applied Superconductivity, vol. 30, no. 6, Sept. 2020, URL: https://ieeexplore.ieee.org/document/9086768

[21] K. Rajashekara, B. Akin, "*Cryogenic Power Conversion Systems: The next step in the evolution of power electronics technology*," IEEE Electrification Magazine, vol. 1, no. 2, Dec. 2013, URL: https://ieeexplore.ieee.org/document/6749061

[22] A. Elwakeel, *et. al.*, "*Study of Power Devices for Use in Phase-Leg at Cryogenic Temperature*," IEEE Transactions on Applied Superconductivity, vol. 31, no. 5, Aug. 2021, URL: https://ieeexplore.ieee.org/document/9372804

[23] H. Gui, *et. al.*, "*Review of Power Electronics Components at Cryogenic Temperatures*," IEEE Transactions on Power Electronics, vol. 35, no. 5, May 2020, URL: https://ieeexplore.ieee.org/document/8854889

[24] H. Gui, *et. al.*, "*Development of High-Power High Switching Frequency Cryogenically Cooled Inverter for Aircraft Applications*," IEEE Transactions on Power Electronics, vol. 35, no. 6, June 2020, URL: https://ieeexplore.ieee.org/document/8883075

[25] L. Nela, *et. al.*, "*Performance of GaN Power Devices for Cryogenic Applications Down to 4.2 K*," IEEE Transactions on Power Electronics, vol. 36, no. 7, July 2021, URL: https://ieeexplore.ieee.org/document/9309188

[26] R. Chen, F. F. Wang, "*SiC and GaN Devices With Cryogenic Cooling*," IEEE Open Journal of Power Electronics, vol. 2, pp. 315-326, April 2021, URL: https://ieeexplore.ieee.org/document/9411696

[27] C. B. Barth, *et. al.*, "*Design, Operation, and Loss Characterization of a 1-kW GaN-Based Three-Level Converter at Cryogenic Temperatures*," IEEE Transactions on Power Electronics, vol. 35, no. 11, Nov. 2020, URL: https://ieeexplore.ieee.org/document/9075366

[28] J. L. Felder, *et. al.*, "*Turboelectric Distributed Propulsion in a Hybrid Wing Body Aircraft*," NASA Glenn Research Center, 2011, URL: https://ntrs.nasa.gov/api/citations/20120000856/downloads/20120000856.pdf?attachment=true

[29] C. E. Jones, *et. al.*, "*Comparison of Candidate Architectures for Future Distributed Propulsion Aircraft*," IEEE Transactions on Applied Superconductivity, vol. 26, no. 6, Sept. 2016, URL: https://ieeexplore.ieee.org/document/7407568

[30] F. Berg, *et. al.*, "*HTS Electrical System for a Distributed Propulsion Aircraft*," IEEE Transactions on Applied Superconductivity, vol. 25, no. 3, June 2015, URL: https://ieeexplore.ieee.org/document/7024922